SPECTRUM OF LUMINESCENCE FROM LASER-INDUCED BUBBLES IN WATER AND CRYOGENIC LIQUIDS

Ohan Baghdassarian, Han-Ching Chu, Bernd Tabbert, and Gary A. Williams

Department of Physics and Astronomy, University of California, Los Angeles, CA 90095

Abstract

The spectrum of the luminescence pulse from collapsing laser-induced bubbles in water and cryogenic liquids has been measured. For small bubbles in water the spectrum approximates that of a black-body at about 7800 K, while for bubbles whose maximum radius is greater than 1 mm the OH* molecular band at 310 nm becomes apparent, a feature which is also seen in multi-bubble sonoluminescence. The larger bubbles also show considerable instabilities in the vicinity of the collapse minimum, where jets and fission events are observed. In the liquid nitrogen and liquid argon the the luminescence is found to consist of discrete lines from chromium atoms, which are compressed in the bubble collapse to a temperature of about 4500 K. The chromium apparently results from the vaporization by the laser of stainless steel microparticles floating in the liquids, possibly knocked off the cell walls by the strong shock waves generated by the laser focusing.

1 Introduction

The mechanism which produces luminescence pulses from collapsing bubbles is still not well understood. The compression of the gas in the bubble can produce fairly high temperatures, but exactly how the light is produced remains controversial (Putterman 2001 and Hilgenfeldt 2001). There are also significant unexplained differences between multibubble and single-bubble sonoluminescence (MBSL and SBSL). In MBSL an emission band from OH* at 310 nm is observed in the spectrum of the luminescence (Matula 1995), whereas SBSL shows only a featureless spectrum rising smoothly into the ultraviolet (Hiller 1995). To try to understand better the nature of the light emission, we have undertaken studies of the light emission from freely-collapsing bubbles in water and in cryogenic liquids. The bubbles are created from a focused laser pulse, which allows the study of bubbles whose maximum radius is between 0.2 and 2 mm, considerably larger than the 0.05 mm maximum radius of SBSL bubbles.

2 Apparatus

To create the bubbles a Nd:Yag laser producing 6 ns pulses with a maximum energy of 600 mJ at 1064 nm is collimated and focused to a point about 10 μm in diameter in the sample liquid, as previously described in Baghdassarian 1999, 2000, and 2001. The laser energy is adjusted to the threshold for just creating a single bubble, typically of order 100 mJ. For the water sample the sealed cell has quartz windows for monitoring the emitted light with a photomultiplier, and the radius of the bubble versus time is monitored by a shadowgraph technique and by pulsed-laser photography through a long-distance microscope. To analyze the spectrum, the light emitted from the bubble region is collected and collimated by a MgF_2-coated paraboloidal mirror. A second paraboloid mirror focuses the collimated beam into the entrance slits of a 0.3 m spectrometer with a gateable intensified CCD detector. To reject light at higher order, long-pass filters at either 300 nm or 500 nm are placed in front of the spectrometer. The spectral response from 200–800 nm is calibrated for detection efficiency against a tungsten-halogen lamp and a deuterium lamp, with and without the cell in place to correct for the absorption of the water and windows. Two different gratings are used, having a spectral range on the ICCD detector of about 200 nm (2 nm resolution) and 30 nm (0.3 nm resolution), respectively. To get sufficient signal for a spectrum it is necessary to average the light from 40–50 bubbles

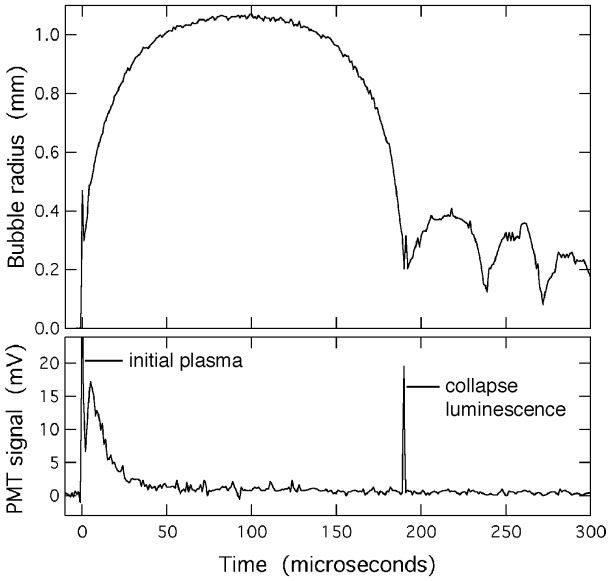

Figure 1: a) Bubble radius in water at atmospheric pressure, and light signal versus time.

over a small range of bubble sizes. The water in the cell is triple-distilled and deionized (resistance 18 MΩ), and has been passed through a 0.22 μm filter. For some measurements it is left with the ambient air dissolved in it; for other runs it is first pumped with a mechanical pump through a nitrogen cold trap for several hours while being circulated with a magnetic stirrer. It is then either left degassed, or a desired partial pressure of gas is introduced.

For the experiments with liquid argon and liquid nitrogen a vari-temp optical dewar is employed to cool the sample chamber to the range 65–90 K. The temperature is maintained constant with a feedback heater to within 0.1 K. The sample cell is constructed of 304 stainless steel whose surface was anodized black to minimize reflections. The quartz windows in the cell are sealed with indium O-rings, and the cell can be pressurized to more than 30 bars. The sample liquids are condensed into the cell from high-purity (5N) gas bottles.

3 Water Results

Fig. 1 shows the growth and collapse of a bubble in ambient 1 bar degassed water after it is created with the laser pulse, as monitored with the shadowgraph technique. A sharp luminescence pulse is observed precisely at the collapse point of the bubble. We find (Baghdassarian 1999) that the width of the emission pulse is several nanoseconds, and it increases linearly as the bubble size increases, shown in Fig. 2. This is quite consistent with the shorter pulse widths (150–300 ps) found for the smaller bubbles of SBSL (Gompf 1997, Hiller 1998), shown as the rectangle in the figure. We also observe that when the water is pressurized a shape instability causes the bubble to split in two just before the collapse point, and each of those bubbles then radiates light. A further finding is that the luminescence is independent of any dissolved gases in the water, in sharp contrast to the high sensitivity found for SBSL.

We can photograph the collapsing bubble with a series of fast laser pulses, shown in Fig. 3, where the bright spot at the center is the luminescence pulse at the minimum radius. Figure 3 c) shows an enlarged view of the luminescing hot spot, which is about 25 μm in diameter, in agreement with previous studies (Ohl 1998). The rebound of the bubble just past the minimum radius is always seen to be highly distorted, and occasionally sharp jet-like structures are seen such as in Fig. 3 b). We have been able to measure the spectrum of the luminescence from the collapse point for bubbles with radius between 0.6–0.8 mm, shown in Fig. 4 (Baghdassarian 2001). The spectrum can be fit to blackbody radiation at a temperature of about

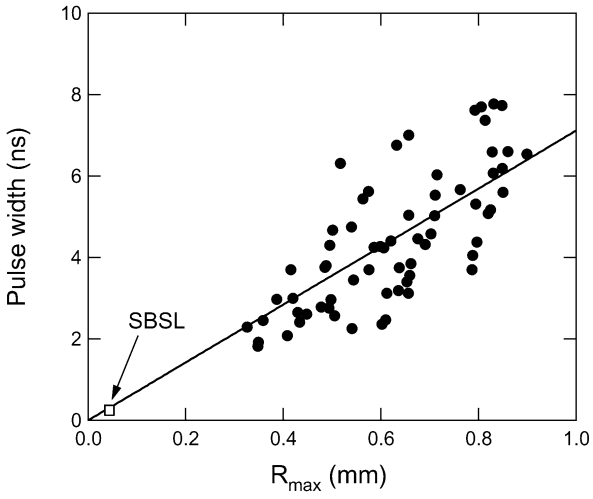

Figure 2: Pulse width versus maximum bubble radius.

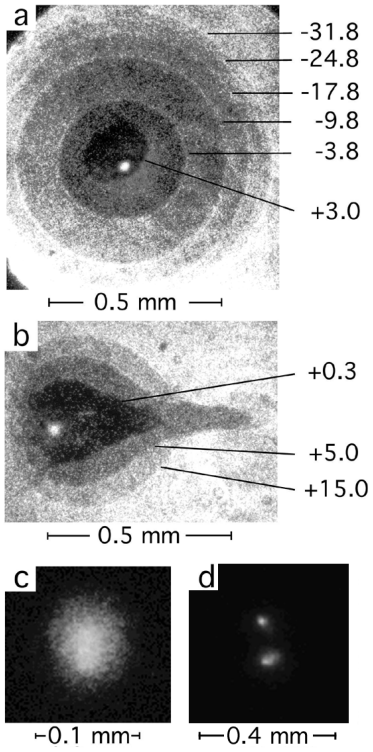

Figure 3: Photographs of the bubbles, backlit with 200 ns pulses from an Ar-ion laser. a) The luminescence from the hot spot is visible in the center of a collapsing bubble of maximum radius 0.45 mm, shown for five exposures on the collapse (negative times in μs from the luminescence pulse at 92 μs) and one on the asymmetric rebound (positive time), b) Three exposures of a bubble after the collapse point, showing the formation of a jet-like structure on the rebound. c) Enlarged view of the luminescence hotspot from a bubble with 0.8 mm maximum radius. d) Double flash from a split bubble of maximum radius 1 mm.

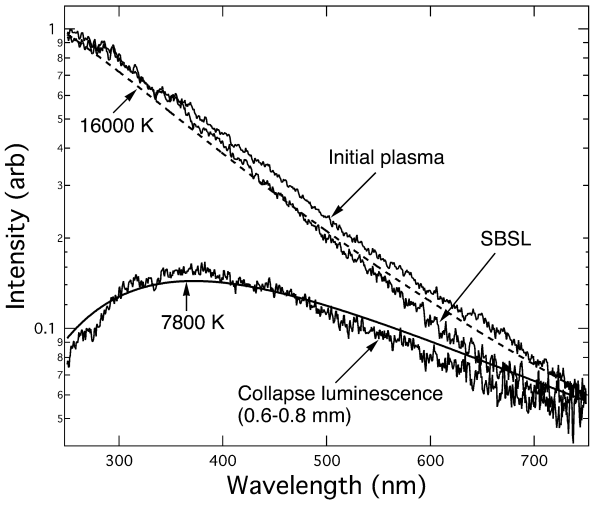

Figure 4: Spectral intensity versus wavelength for the luminescence from small bubbles (0.6–0.8 mm maximum radius), from the initial laser-induced plasma, and from an SBSL cell positioned at the point where the laser bubbles are created. Intensities have been scaled arbitrarily between the different curves.

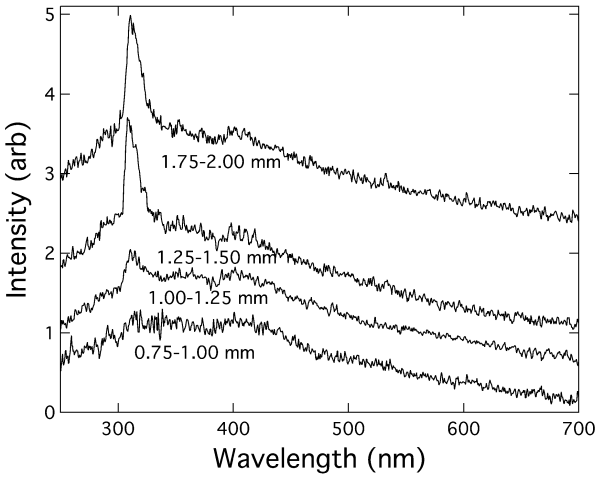

Figure 5: Spectra of the collapse luminescence as the bubble size is increased, showing the growth of the OH* band at 310 nm. These are averaged over 40–50 bubbles having maximum radii in the range indicated, and have been offset in the vertical direction to separate them (they are normalized to all coincide with the lowest curve between 500–700 nm).

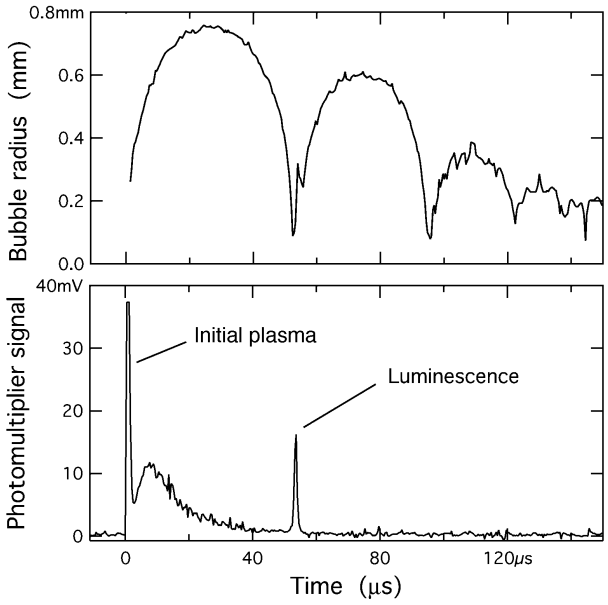

Figure 6: bubble radius versus time and light emission from a bubble in liquid nitrogen at 66 K and 5.8 bar

7800 K (solid curve). This spectrum is compared to that of single-bubble sonoluminescence (150 torr air in water) and to the light emitted from the plasma created in the initial laser pulse ionizing the water. These curves appear to have a nearly identical wavelength dependence, and are characterized by a higher temperature, of order 16,000 K (dashed curve).

The luminescence spectra from larger bubbles is shown in Fig. 5 For bubbles larger than about 1 mm maximum radius we find that the spectrum contains also a discrete line emission at 310 nm from the OH* molecular band. This line is also observed in the spectrum of multibubble sonoluminescence (Matula 1995). In the larger bubbles we also find that surface instabilities at the collapse point become very frequent, often causing the bubble to split into two bubbles just before the collapse, both of which still emit light, as shown in Fig. 3 d). Since the OH* line becomes evident at about the same bubble sizes where the instabilities begin occurring, we surmise that there may well be a connection between the two phenomena, although the exact mechanism for this is unclear.

4 Cryogenic Liquid Results

When the same laser-focusing experiment is carried out in liquid nitrogen or liquid argon pressurized to 3–5 bars (Baghdassarian 2000), we also observe a luminescence pulse at the collapse point of the bubble, but with a number of features different from the water case. Figure 6 shows the bubble radius versus time, and the luminescence pulse at the collapse point. The luminescence has an integrated intensity of up to 10^{10} photons, about two orders of magnitude larger than seen from the laser bubbles in water, and three orders of magnitude larger than the maximum intensity of SBSL. This is probably related to the fact that the width of the pulse ranges from 200–1000 ns, depending on the bubble size, a factor of 100 longer than the pulse widths found in water (Fig. 7)). The longer pulse width indicates slower dynamics at the collapse point than in water bubbles, which is consistent with the large rebound amplitude of the bubble motion in Fig. 6. With a slower collapse region less energy will be radiated as a shock wave, leading to a more elastic rebound. Photographs of the emission spot show that it is larger than in water, on the order of 70 μm.

We have measured the spectrum of the luminescence from bubbles in liquid nitrogen and argon, with very surprising results. We see discrete atomic lines in the spectra, shown in Fig. 8, an indication that the gas density in the bubble must be considerably lower than those in water. The wavelengths of the lines turned out to be precisely the same for bubbles in both liquid nitrogen and liquid argon, with no argon or nitrogen

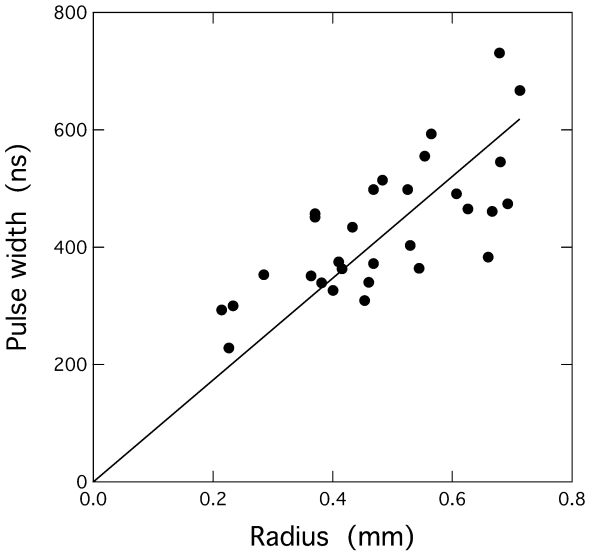

Figure 7: Luminescence pulse width in liquid nitrogen versus maximum bubble radius

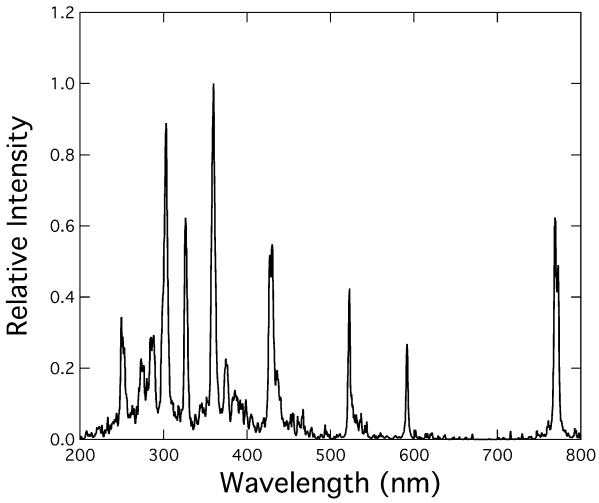

Figure 8: Spectrum of the collapse luminescence in liquid argon at 87 K, 4.5 bars pressure

emission lines. By matching with atomic tables we find that most of the lines can be identified as coming from excited states of the chromium atom. This must arise from microscopic particles (i.e. 100–1000 Å) of stainless steel floating in the cryogenic liquids, which would be preferentially vaporized by the incident laser pulse. At this point we do not know the exact origin of the stainless steel flakes, but guess that they are being dislodged from the stainless walls of our cell by the shock waves generated with each laser pulse.

The chromium line at 430 nm in Fig. 8 is actually three closely spaced lines, as shown in the high-resolution scan of Fig. 9. Since the relative amplitude of these lines depends on the population of the upper levels, it is possible to extract the temperature to which the chromium atoms are being heated in the bubble collapse. Weighting the Boltzmann factors by the degeneracies of the levels, a fit to the observed amplitudes yields a temperature of about 4500 K.

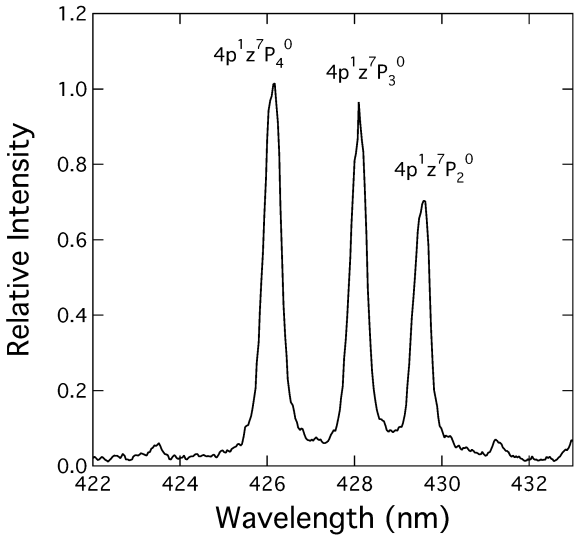

Figure 9: High-resolution spectrum of chromium emission lines near 430 nm, labelled by the upper 4p states.

Acknowledgements

Work supported by the National Science Foundation, DMR 97-31523, and in part by DARPA, funded through the ONR, SOT division. One of us (B. T.) wishes to thank the Deutsche Akademie der Naturforscher Leopoldina for fellowship support.

References

O. Baghdassarian, B. Tabbert, and G. A. Williams, *Phys. Rev. Lett.* **83**, 2437 (1999).

O. Baghdassarian, B. Tabbert, and G. A. Williams, *Physica B* **284–288**, 393 (2000).

O. Baghdassarian, H. Chu, B. Tabbert, and G. A. Williams, *Phys. Rev. Lett.* **84**, 4934 (2001).

B. Gompf, R. Gunther, G. Nick, R. Pecha, and W. Eisenmenger *Phys. Rev. Lett.* **79**, 1405 (1997).

S. Hilgenfeldt, S. Grossman, and D. Lohse, *Nature* **409**, 783 (2001).

R. Hiller and S. Putterman, *Phys. Rev. Lett.* **75**, 3549 (1995);

R. Hiller, K. Weninger, and S. Putterman, *Phys. Rev. Lett.* **80**, 1090 (1998);

T. Matula, R. Ronald, P. Mourad, W. McNamara, and K. Suslick, *Phys. Rev. Lett.* **75** 2602 (1995).

C. Ohl,T. Kurz, R. Geisler, O. Lindau, and W. Lauterborn, *Phil. Trans. R. Soc. Lond.* A **357**, 269 (1999).

S. Putterman, P. Evans, G. Vasquez, and K. Weninger, *Nature* **409**, 782 (2001).